Progress In Electromagnetics Research C, Vol. 83, 147–159, 2018

Design and Analysis of Hetero Triangle Linked Hybrid Web Fractal Antenna for Wide Band Applications

Bandhakavi S. Deepak, Boddapati T. P. Madhav*, Vinnakota S. V. Prabhakar, Pappula Lakshman, Tirunagari Anilkumar, and Manikonda Venkateswara Rao

Abstract—Design and analysis of a novel wide-band covering, hetero triangle linked hybrid web fractal antenna is presented in this paper. The hetero triangle linked hybrid web structure has been designed through multiple iterations in the CST MICROWAVE STUDIO electromagnetic simulation tool and has been fabricated on FR4 dielectric of $\varepsilon_r = 4.4$ with height of 1.6 mm. The proposed antenna offers a comprehensive bandwidth of 18.055 GHz, covering from 1.945 GHz to 20 GHz. It supports various applications starting from 3G, LTE, ISM, Bluetooth, Wi-Fi, WLAN (2.4–2.48 GHz) and 5.2/5.8 GHz (5.15–5.35 GHz/5.72–5.82 GHz), WiMAX operating in the 2.3/2.5 GHz (2.305–2.36 GHz/2.5–2.69 GHz), 5.5 GHz (5.25–5.85 GHz) and Satellite communication (Ku band: Uplink of 14 GHz and Downlink of 10.9–12.75 GHz). The proposed antenna provides peak realized gain of 7.17 dB with efficiency more than 78% in the operating band. The antenna parameters such as reflection coefficient, gain and radiation patterns are determined through numerical simulation, and good matching is obtained with measured results.

1. INTRODUCTION

Nowadays, the significance of fractal antennas in extracting greater bandwidths with compact size has become tremendously appreciable. The concept of fractals has been playing an inspiring role during a few decades in the antenna design. They have the ability to create multi-band and wideband performance with their self-similar and space-filling properties, also mentioned as an object generated recursively with fractional dimension. The radiation phenomenon of the fractal shapes shall be determined by the existence of actively concentrated surface currents that travel along the interconnected self-similar units. As the need for wide and ultra-wideband covering antennas is creeping up day by day, the fractal antennas have occupied the driving seat in offering wider bandwidths with adequate efficiencies and gains. Therefore, it has set the trend in achieving wider bandwidths for multiple applications. Good amount of research has already been done on the fractal geometry based microstrip antennas, and many researchers have proposed various novel fractal geometries offering wider bandwidths. Best [1] proposed a Sierpinski gasket fractal antenna for multiband behaviour of Sierpinski gasket as a function of the periodic placement of four gaps located along with the central vertical axis of the antenna. Anagnostou [2] proposed a coplanar waveguide fed Koch dipole slot antenna for ISM frequency band applications. The dimensions of the antenna are optimized to achieve the compactness with the placement of fractal shapes at the radiating slots. Best [3] proposed a comparison of the resonant properties in space filling fractal antennas. He demonstrated the resonant properties w.r.t antenna geometry and total wire length. Venkata Kiran [4] proposed a compact dual-element rectangular DRA with combination of Sierpinski and Minkowski fractals to reduce the size suitable for wideband applications.

Received 12 March 2018, Accepted 9 April 2018, Scheduled 17 April 2018

* Corresponding author: Boddapati Taraka Phani Madhav (btpmadhav@kluniversity.in).

The authors are with the Antennas and Liquid Crystals Research Centre, Koneru Lakshmaiah Education Foundation, Vaddeswaram, AP, India.

Mukherjee [5] designed a hemispherical DRA based on apollonian gasket of circles on ceramic thermoset polymer composite material. The design model projected impedance bandwidth of around 47% at resonant frequency of 3.6 GHz.

Gupta and Mathur [6] proposed a Koch fractal-based hexagonal patch antenna for circular polarization working in 6–11 GHz with 58.82% bandwidth. Trivedi and Pujara [7] proposed a wideband fractal tetrahedron dielectric resonator antenna with triangular slots operating in 3.8–8.1 GHz and achieved an impedance bandwidth about 72.3%. Mukti et al. [8] proposed a compact fractal wideband planar antenna for L-band applications with a meandered transmission line structure covering 0.94–2.25 GHz with 82.13% bandwidth. Srivastava et al. [9] proposed the design of a wideband square fractal antenna with gap coupling, operating in the band of 1.68–4.07 GHz with an impedance bandwidth of 83.13%. Elsheakh and Abdallah [10] proposed an ultrawide bandwidth monopole antenna for DVB-T and wireless applications operating from 4–10.6 GHz with 85.71% bandwidth. Sankaranarayanan et al. [11] proposed a novel compact cylindrical dielectric resonator antenna with fractal ring in 4.7–12.4 GHz with 90% bandwidth.

Susila et al. [12] proposed a novel smiley fractal antenna along with N-notch design for ultra wideband applications operating in 3.24–11.14 GHz and achieved 109% bandwidth. Kaka and Toycan [13] proposed a hexagonal Sierpinski gasket antenna with multiband characteristics for UWB wireless communication applications operating in 3.1–10.6 GHz with 109.48% bandwidth. Lin and Chuang [14] proposed a 3–12 GHz UWB planar triangular monopole antenna with ridged ground plane with 120% bandwidth. Tizyi et al. [15] proposed a CPW and microstrip line fed compact fractal antenna for UWB-RFID applications working in 3.4–16.4 GHz with 131.31% bandwidth. Kumar and Gaikwad [16] proposed a nanoarm fractal antenna for UWB applications (2.55–11.84 GHz) with 131.77% bandwidth.

Madhav et al. [17] proposed an asymmetric LCP fractal UWB monopole slotted antenna with notching from 3.7716 GHz to 4.07 GHz. Wang et al. [18] proposed a compact UHF antenna based on complementary fractal technique operating from 0.7 GHz to 4.71 GHz. Hu et al. [19] proposed a novel rectangle tree fractal UWB antenna with dual band-notched characteristics operating in 3–11 GHz with two notch bands at 3.3–4.08 GHz and 5.04–6.03 GHz, respectively. Lincy et al. [20] proposed a wideband fractal micro-strip antenna for wireless application.

In this paper, we propose a hetero triangle linked hybrid web fractal microstrip patch antenna which offers an impedance bandwidth of about 164.55% operating in 1.945–20 GHz frequency band with peak realized gain of more than 7.1 dB.

2. DESIGN AND ANALYSIS

A novel hetero triangle linked hybrid web fractal antenna using an FR4 substrate is an intellectual design, which is an attempt made to enhance the operating bandwidth. Fortunately, the novelty in design has turned up quite well with some astonishing results, and there is a very good agreement between the simulated and practical results as well. The entire design has been realized through four iterations where different types of triangles are linked together in the form of a hybrid web. In the first iteration, two equilateral triangles, four isosceles triangles and eight scalene triangles of distinct dimensions are joined together symmetrically in such a way that a hexagonal ring of dimensions 4 mm and 7.8 mm (shorter and longer dimensions, respectively) is formed. In the second iteration, two isosceles triangles and eight scalene triangles are linked together symmetrically in such a way that a concentric hexagonal ring of dimensions 2 mm and 4.6 mm (shorter and longer dimensions, respectively) is produced. The third iteration is the combination of the 2nd iteration with diminished dimensions and the optimised version of the same along with a circularly perforated equilateral triangle inserted at the centre.

Iteration wise constructive design of hetero triangle linked hybrid web fractal microstrip antenna is shown in Fig. 1.

Initially, the basic shape (iteration-0) which is a circular ring with an outer radius of 12 mm and inner radius of 9.4 mm (optimised) forming a ring width of $R = 2.6$ mm is designed using the CST electromagnetic software. The radius 'a' is calculated using the relation

$$a = F/f1 + [2h/\pi\varepsilon_r F]\,[\ln(\pi F/2h) + 1.7726]\,g^{1/2} \tag{1}$$

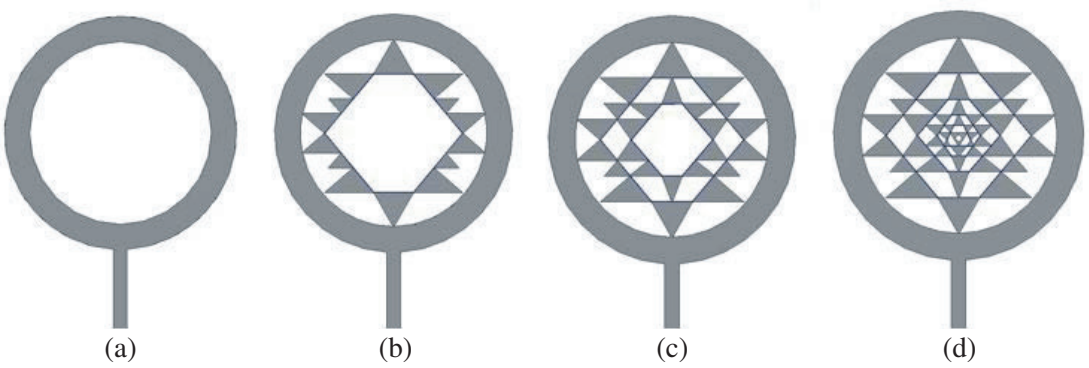

Figure 1. Hetero triangle linked hybrid web fractal antenna design, (a) basic shape, (b) iteration-1, (c) iteration-2, (d) iteration-3.

$$\text{where, } F = \left[8.791 \times 10^9\right] \Big/ \left[f_r(\varepsilon_r)^{1/2}\right] \tag{2}$$

'f_r' is the resonant frequency (Hz), 'ε_r' the relative permittivity of dielectric substrate, 'h' the height of the substrate (cm), and 'w' the width of the feed line. Microstrip line feed is designed for approximately 50 ohm characteristic impedance. The effective dielectric constant 'ε_{eff}' is calculated based on 'ε_r'.

$$\varepsilon_{\text{eff}} = \frac{\varepsilon_r + 1}{2} + \frac{\varepsilon_r - 1}{2} \frac{1}{\sqrt{1 + 12\dfrac{h}{w}}} \tag{3}$$

$$Z_0 = \frac{120\pi}{\sqrt{\varepsilon_{\text{eff}}\left[\dfrac{w}{h} + 1.393 + 0.667 \ln\left(\dfrac{w}{h} + 1.444\right)\right]}}, \quad \text{for } w/h > 1 \tag{4}$$

The motivation behind the design of the proposed fractal antenna is the "Sri-Chakra", which is the fundamental archetype of the universe as per the Hindu mythology. Hence the fractal iterations are considered as per a 2D Sri-Chakra structure. In the first iteration, two equilateral triangles with T1 dimensions, four isosceles triangles with T4 dimensions and eight scalene triangles with T2 and T3 dimensions respectively are placed around a hexagon in such a way that the two equilateral triangles are arranged symmetrically on the smaller dimensions of the hexagon (4 mm), and the remaining 12 triangles are arranged symmetrically on the larger dimensions of the hexagon (7.81 mm) as shown in Fig. 2. The vertices of triangles with dimensions T1 and T3 intersect the inner circle at six different points, where the phase difference between the two symmetric points with respect to the centre is 180°.

In the second iteration, two isosceles triangles with T5 dimensions and eight scalene triangles with T6 and T7 dimensions are placed on a hexagon of 2 mm and 4.6 mm (shorter and longer dimensions, respectively), where the shorter dimensions of the hexagon are occupied with the bases of two isosceles triangles, and the remaining eight scalene triangles occupy the longer dimensions of the hexagon symmetrically. One vertex of each triangle in the second iteration intersects with the first iteration hexagon, in order to form a web as shown in Fig. 1(c).

In the third iteration, a total of nineteen triangles are linked together as shown in Fig. 1(d). It is a combination of 2nd iteration with altered dimensions, and it is an optimised version, where five isosceles triangles of T8, T11 and T12 dimensions, three equilateral triangles of T15 and T16 dimensions with T16 being perforated with an incircle of radius 0.3 mm and eleven scalene triangles of T6, T7, T9, T10, T13 and T14 dimensions are latched together in a symmetrical fashion to obtain the design of the hetero triangle linked hybrid web fractal antenna as shown in Fig. 2. For all the triangles, the third side dimensions are calculated by using the pythogorean theorem ($c^2 = a^2 + b^2$) with the help of a median drawn to the base of the triangle, and the angles are calculated using the cosine function ($\cos(\theta)$ = adjacent side/hypotenuse).

The dimensions of all the triangles named as per Fig. 2 and the optimized design parameters of the proposed hetero triangle linked hybrid web fractal antenna are tabulated in Table 1 and Table 2, respectively.

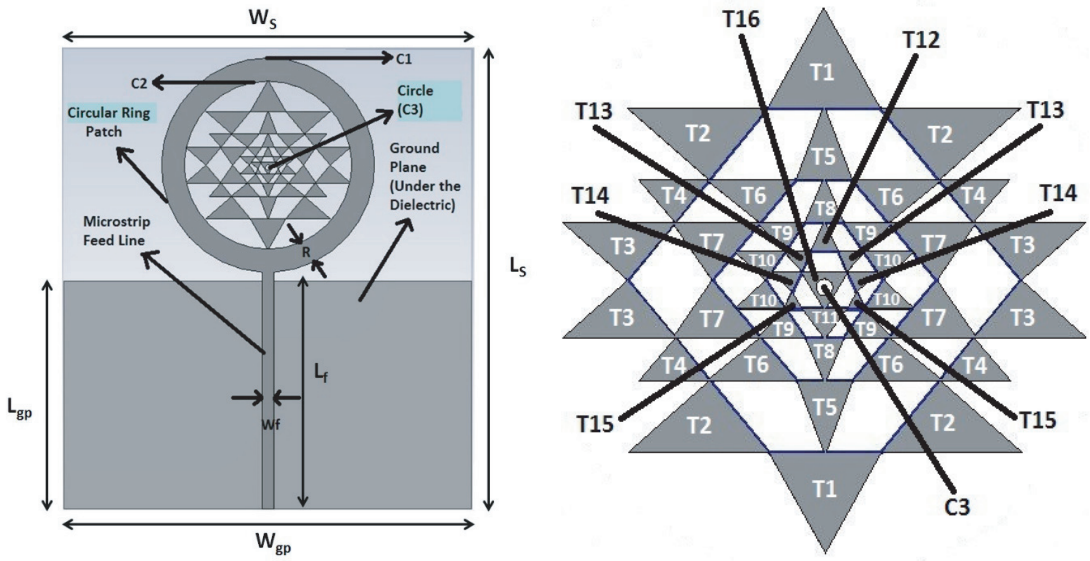

Figure 2. Hetero triangle linked hybrid web fractal antenna along with the interior design.

Table 1. Dimensions of the triangles used in forming the hybrid web structure.

Triangle Name	Triangle Type	Triangle Dimensions		
		Side 1 (mm)	Side 2 (mm)	Side 3 (mm)
T1	Equilateral	4	4	4
T2	Scalene	3.2	3.9	5
T3	Scalene	2.62	3	4
T4	Isosceles	1.98	1.98	2.5
T5	Isosceles	2	2.69	2.69
T6	Scalene	1.98	2.42	3.2
T7	Scalene	2.44	2.62	3.1
T8	Isosceles	1.4	1.74	1.74
T9	Scalene	1.22	1.41	1.7
T10	Scalene	1.22	1.48	1.8
T11	Isosceles	1.6	1.74	1.74
T12	Isosceles	1	1.16	1.16
T13	Scalene	0.76	0.95	0.955
T14	Scalene	0.78	1.06	1.15
T15	Equilateral	0.67	0.67	0.67
T16	Equilateral	1.7	1.7	1.7

3. RESULTS AND DISCUSSION

The optimized design of the proposed antenna is simulated using the CST Microwave simulation software, and the corresponding results of S-parameter, gain, radiation pattern and efficiency are analysed. In the process of optimization, various parameters such as inner circle radius of the circular ring monopole, width of the feed line and length of the ground plane have been altered, and the respective parametric plots are illustrated. The proposed antenna is the third iteration of the basic shape (iteration-0), whose return loss characteristics are optimal compared to the other two iterations

Table 2. Optimized design parameters of the proposed antenna.

Description of the parameter	Value in mm	Description of the parameter	Value in mm
Width of the Substrate, W_s	46	Width of the Ground Plane, W_{gp}	46
Length of the Substrate, L_s	52	Width of the circular ring, R	2.6
Thickness of the Substrate, K	1.6	Radius of outer circle, $C1$	12
Length of the Feed Line, L_f	27	Radius of inner circle, $C2$	9.4
Width of the Feed Line, W_f	1.4	Radius of perforated incircle, $C3$	0.3
Length of the Ground Plane, L_{gp}	26		

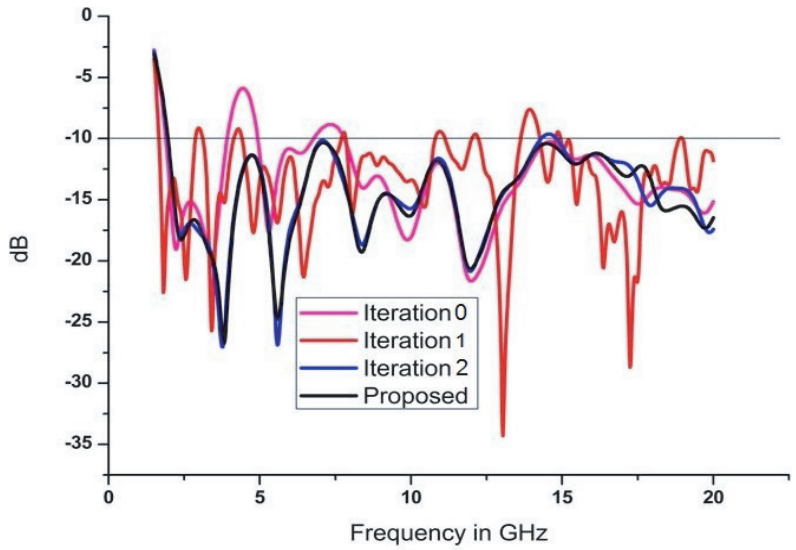

Figure 3. Return loss comparison plot.

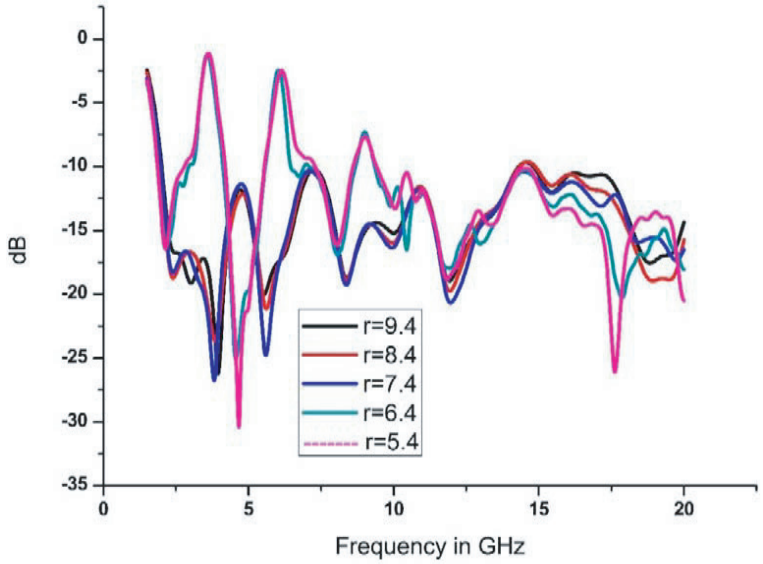

Figure 4. Return loss parametric plot of the inner circle radius.

and the basic shape. In fact, only iteration-3 (proposed antenna) return loss characteristics cover the entire bandwidth completely, whereas the other iterations have notches (over the −10 dB) in their respective return loss characteristics as shown in Fig. 3.

Figure 4 presents the return loss parametric plot for the inner circle radius of the circular monopole where the S-parameter characteristics at different radii have been put together for analysing and picking the optimal inner circle radius. Although return loss characteristics of 8.4 mm and 7.4 mm radii seem a bit better than that of 9.4 mm radius, the former radii overlap with the interior hybrid web design. Therefore, 9.4 mm has been considered as the optimum choice, to nurture the hybrid web structure present inside the circular ring monopole.

The S-parameter parametric plot of the feed line width is as shown in Fig. 5. The return loss characteristics for three distinct feed line widths are compared, where the obvious choice of the optimum feed line width is 1.4 mm whose return loss characteristics are lying strictly under −10 dB throughout the operating frequency band, unlike the other two cases.

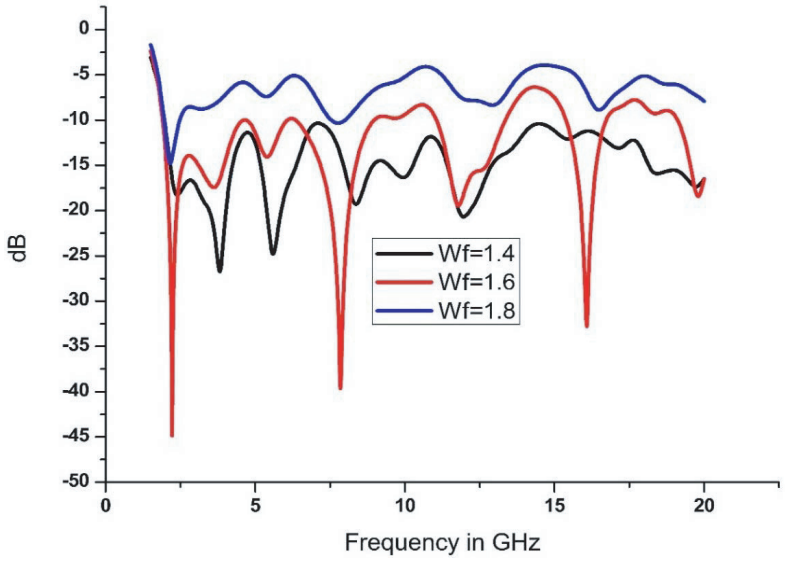

Figure 5. Return loss parametric plot of the feed line width.

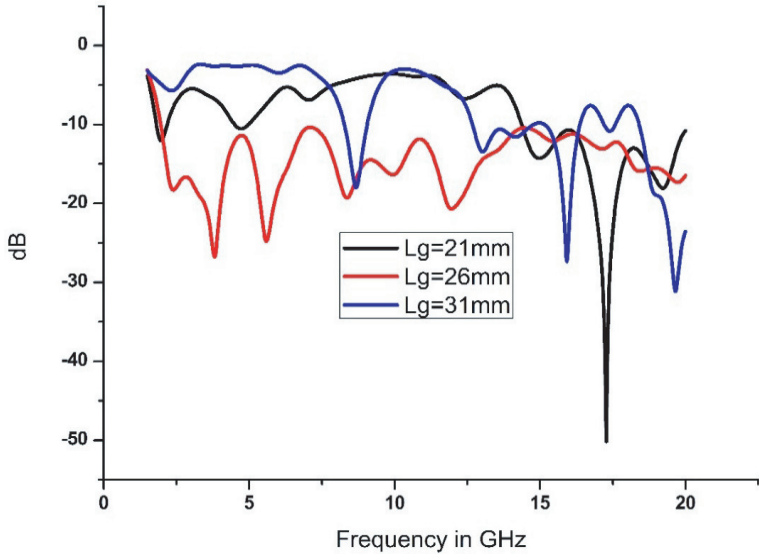

Figure 6. Return loss parametric plot of the ground plane length.

Figure 6 shows the return loss parametric plot for the length of the ground plane where the best possible result in terms of return loss, i.e., under −10 dB throughout the entire band of operation is achieved when the ground plane length (26 mm) is exactly half of the substrate length (52 mm). After performing the parametric analysis on the proposed antenna, the optimum dimensions of inner circle radius are fixed at 9.4 mm, feed line width of 1.4 mm and the ground plane length 26 mm.

Figure 7 shows the gain curve of simulated and measured results, and Fig. 8 shows the efficiency of the antenna in the operating band. An average gain of 5.2 dB and average efficiency of 68% are attained for the current model. The individual peak gain values at different application frequencies in the operating band are also shown in the three-dimensional radiation characteristics plots of Fig. 9. Monopole like radiation is observed in E-plane at lower frequency bands rather than at higher operating

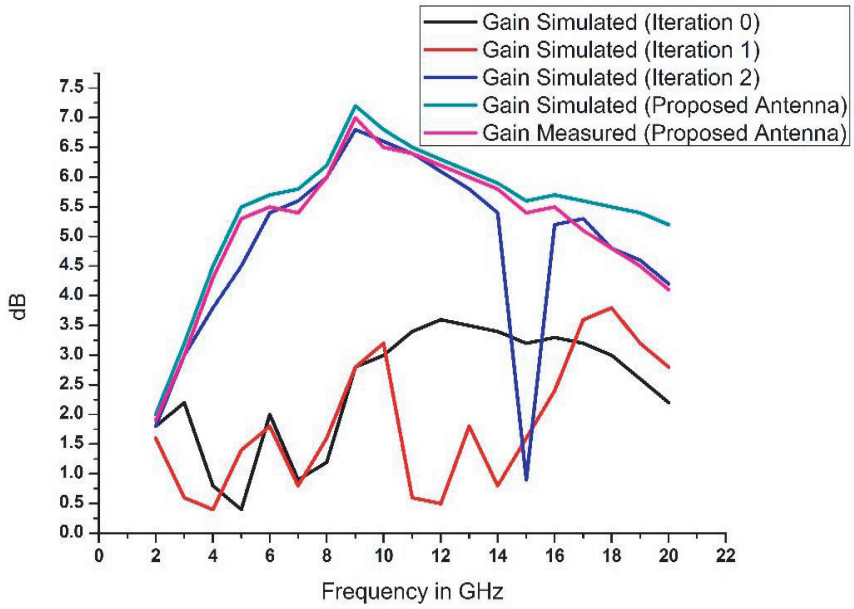

Figure 7. Gain (dB) versus Frequency (GHz) plot.

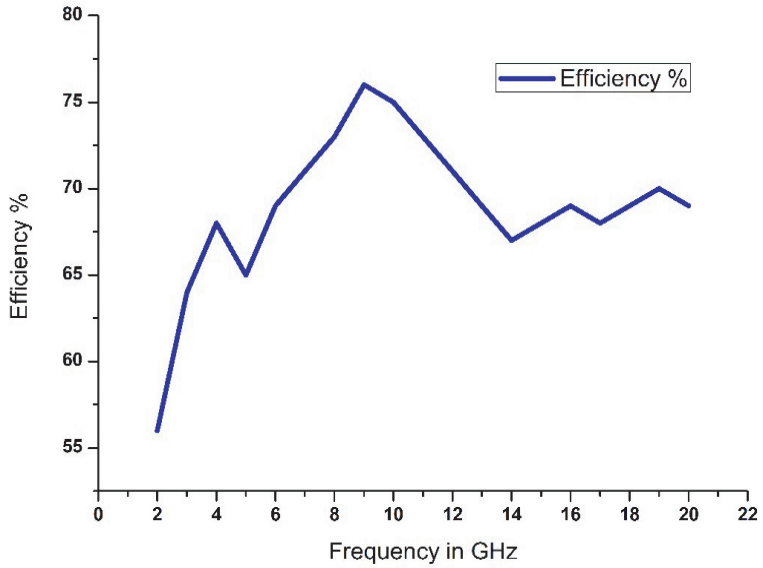

Figure 8. Efficiency versus Frequency plot.

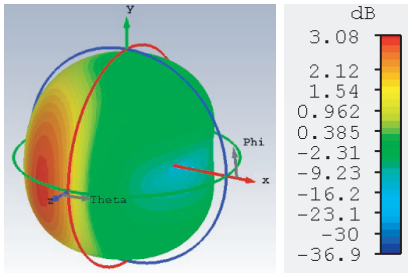

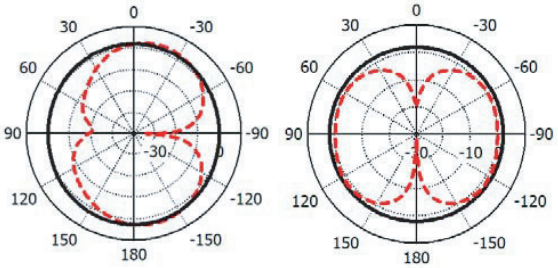

E-plane *H*-plane

(a)

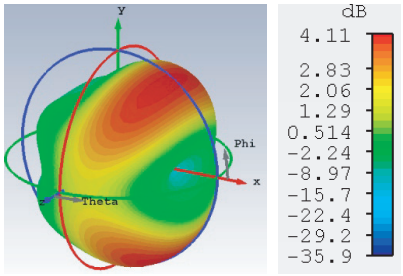

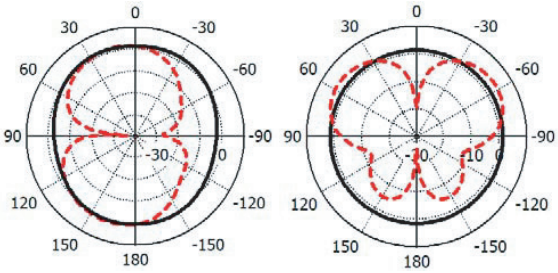

E-plane *H*-plane

(b)

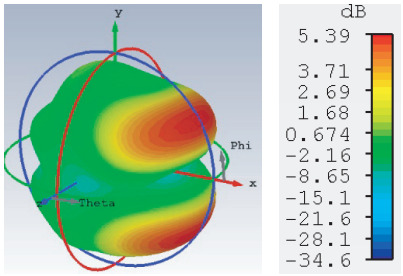

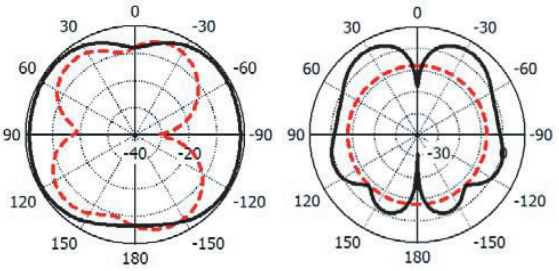

E-plane *H*-plane

(c)

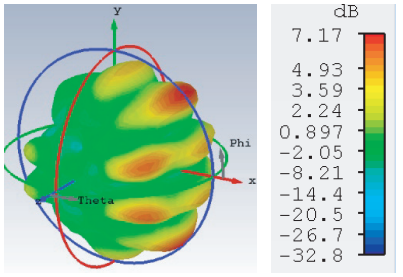

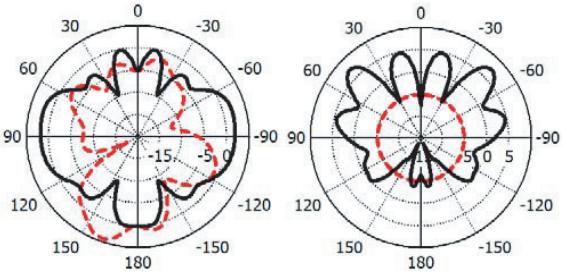

E-plane *H*-plane

(d)

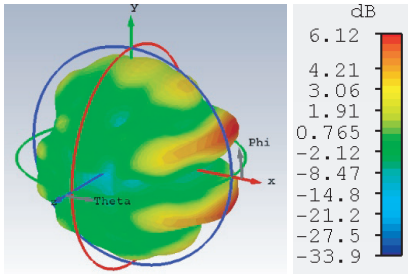

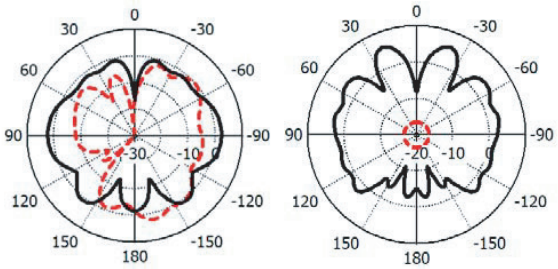

E-plane *H*-plane

(e)

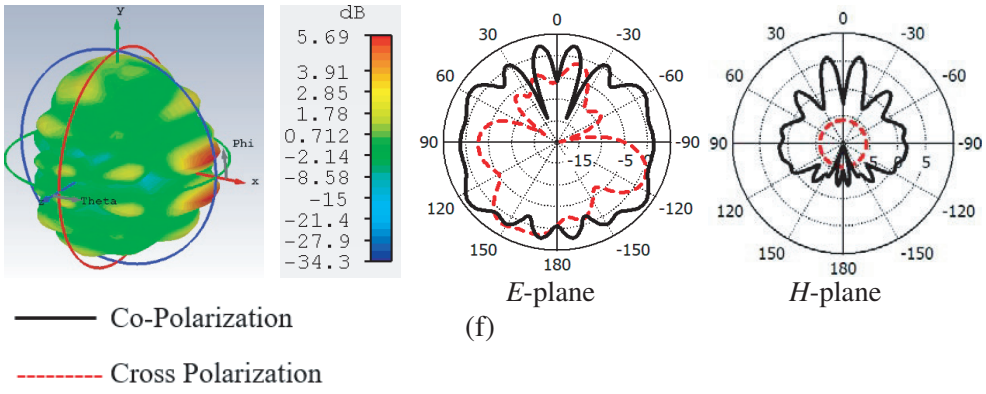

Figure 9. Simulated radiation pattern of the proposed antenna. 3D gain at (a) 2.4 GHz, (b) 3.6 GHz, (c) 5.8 GHz, (d) 9 GHz, (e) 12 GHz, (f) 18 GHz.

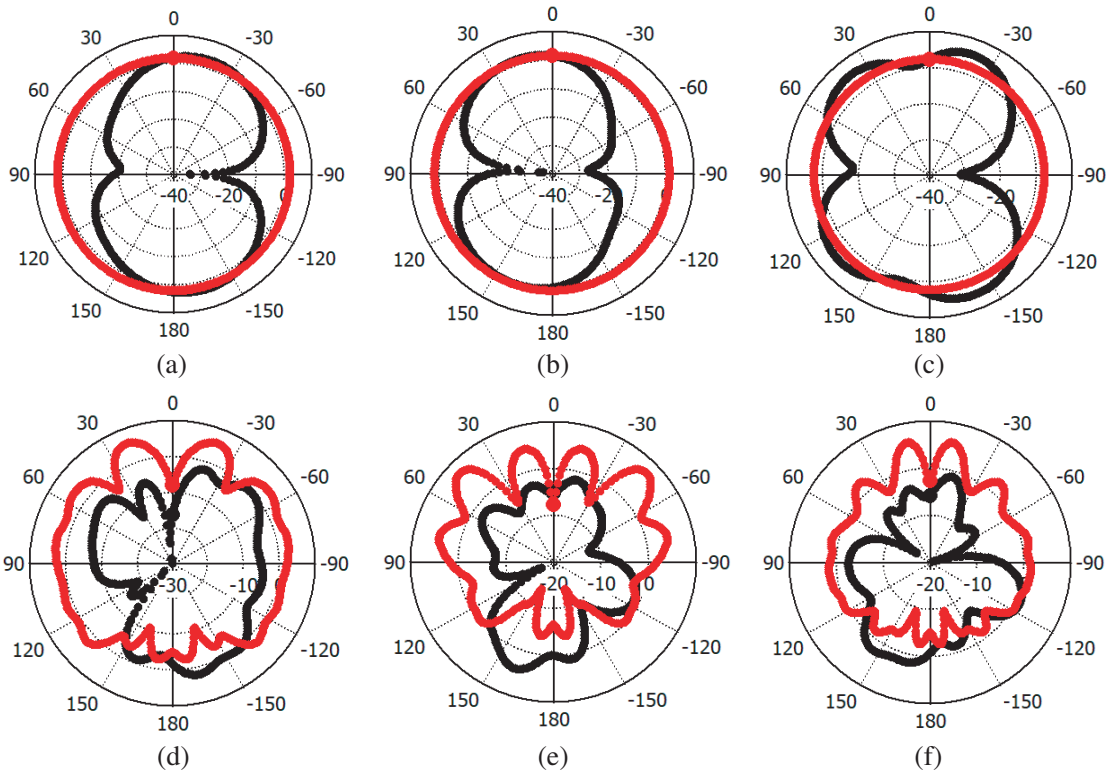

Figure 10. Measured radiation patterns of the proposed antenna, (a) 2.4 GHz, (b) 3.6 GHz, (c) 5.8 GHz, (d) 9 GHz, (e) 12 GHz, (f) 18 GHz.

bands. The cross polarization is low in the H-plane at higher frequency bands and a little bit high at lower bands. The measured radiation patterns of the antenna at identified operating bands are presented in Fig. 10. There is good matching in the measured radiation patterns with simulation results obtained from CST Microwave studio.

Figure 11 shows the current distribution of the antenna at different application bands. At lower operating bands, the maximum current intensity is focused near feed line, and at higher operating bands, the current density is more on feed line as well as on radiating element structure edges.

Parameters of the proposed antenna are compared with those in literature, tabulated in Table 3. As per size is concerned, four models are very compact in nature, but as per the bandwidth is concerned, the

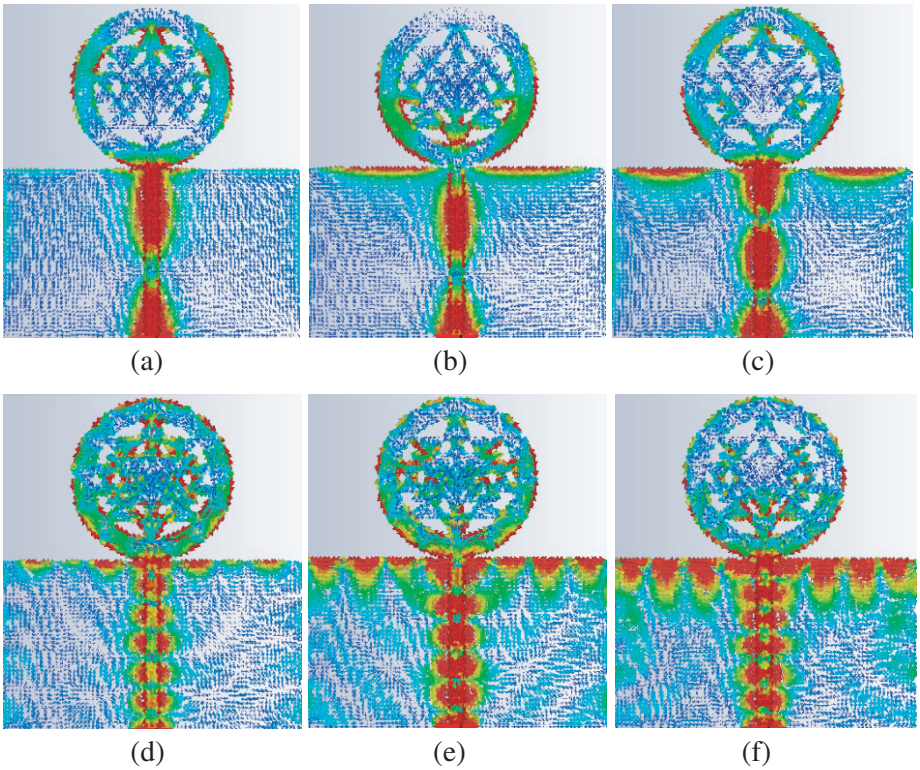

Figure 11. Surface current distribution of the proposed antenna. (a) 2.4 GHz, (b) 3.6 GHz, (c) 5.8 GHz, (d) 9 GHz, (e) 12 GHz, (f) 18 GHz.

Table 3. Comparison of proposed and other antenna designs.

S. No	Reference	Physical Dimensions ($l \times w$ mm^2)	Bandwidth	Peak Gain (dBi)	Impedance Bandwidth (%)	Average Efficiency (%)
1	[4]	80×80	3.52 GHz	6.74	66%	86%
2	[5]	100×100	1.68 GHz	8.5	47%	88%
3	[6]	35×30	5 GHz	4.79	58.82%	62%
4	[7]	140×140	4.3 GHz	7.5	72.3%	72%
5	[10]	80×60	6 GHz	7.6	85.71%	65%
6	[11]	100×100	7.7 GHz	9.13	90%	70%
7	[12]	34×32	7.9 GHz	4.83	109%	66%
8	[13]	48×36	7.5 GHz	4.5	109.48%	64%
9	[20]	31×27	13 GHz	5.75	131.31%	63%
10	Proposed	52×46	18.055 GHz	7.1	164.55%	68%

proposed antenna model provides superior value. A moderate peak realized gain and high impedance bandwidth are obtained with the current model. The designed antenna is fabricated with optimized dimensions after simulation. The front and back views of the prototyped antenna are shown in Fig. 12.

The simulated and measured reflection coefficients of the proposed antenna are shown in Fig. 13. There is an excellent matching observed between the simulation results from CST and measured results on Anritsu combination analyser MS 2037C. Small harmonics can be observed at higher operating bands due to poor soldering in the SMA connector, which does not affect the overall bandwidth and can be neglected.

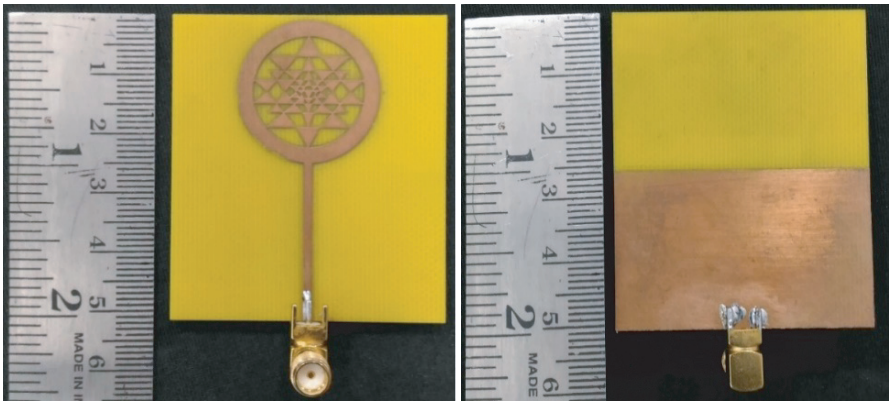

Figure 12. Photograph of the fabricated antenna.

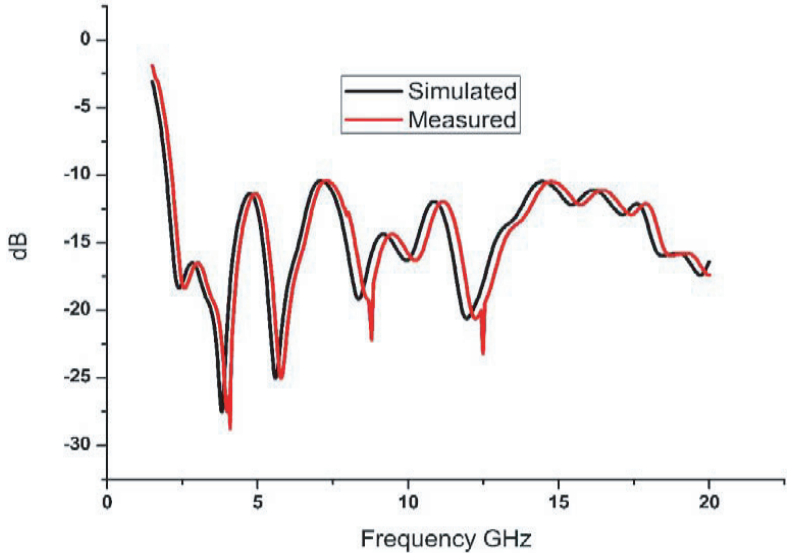

Figure 13. Measured and simulated reflection coefficient.

4. CONCLUSION

A novel, hetero triangle linked hybrid web fractal antenna design has been demonstrated with the possible proofs which highlight the design as well as the analysis aspects. The antenna is designed and optimized through CST Microwave studio, and the corresponding simulated results are presented. The optimized design is fabricated and tested in an anechoic chamber as well as through Anritsu combination analyser. The measured results are also included along with the simulated ones, whose comparison illustrates that there exists a good agreement between them. The proposed antenna offers a broad bandwidth of 18.055 GHz, operating from 1.945 GHz to 20 GHz which covers many applications like 3G, LTE, ISM, Bluetooth, Wi-Fi, WLAN, WiMAX, Satellites (Ku-Band), etc. Peak realized gain of 7.1 dB and peak efficiency more than 78% are the attractive features of the proposed antenna.

ACKNOWLEDGMENT

Authors would like to acknowledge Department of ECE of KLEF and DST through ECR /2016 /000569, and EEQ/2016/000604.

REFERENCES

1. Best, S. R., "On the significance of self-similar fractal geometry in determining the multiband behaviour of the Sierpinski gasket antenna," *IEEE Antennas and Wireless Propagation Letters*, Vol. 1, 22–25, 2002.
2. Anagnostou, D. "A CPW koch dipole slot antenna," *Wireless Communication Technology*, Oct. 15–17, 2003.
3. Best, S. R., "A comparison of the resonant properties of small space filling fractal antennas," *IEEE Antennas and Wireless Propagation Letters*, Vol. 2, 197–200, 2003.
4. Venkata Kiran, D., "Compact embedded dual-element rectangular dielectric resonator antenna combining Sierpinski and Minkowski fractals," *IEEE Transactions on Components, Packaging and Manufacturing Technology*, Vol. 7, No. 5, 786–791, 2017.
5. Mukherjee, B., "Hemispherical dielectric resonator antenna based on apollonian gasket of circles — A fractal approach," *IEEE Transactions on Antennas and Propagation*, Vol. 62, No. 1, 40–47, 2014.
6. Gupta, M. and V. Mathur, "Koch fractal-based hexagonal patch antenna for circular polarization," *Turk. J. Elec. Eng. & Comp. Sci.*, Vol. 25, 4474–4485, 2017.
7. Trivedi, K. and D. Pujara, "Design and development of a wideband fractal tetrahedron dielectric resonator antenna with triangular slots," *Progress In Electromagnetics Research M*, Vol. 60, 47–55, 2017.
8. Mukti, P. H., S. H. Wibowo, and E. Setijadi, "A compact wideband fractal-based planar antenna with meandered transmission line for L-band applications," *Progress In Electromagnetics Research C*, Vol. 61, 139–147, 2016.
9. Srivastava, D. K., A. Khanna, and J. P. Saini, "Design of a wideband gap-coupled modified square fractal antenna," *Journal of Computational Electronics*, Vol. 15, No. 1, 239–247, 2016.
10. Elsheakh, D. M. and E. A. Abdallah, "Design ultra-wide bandwidth monopole antenna for DVB-T and wireless applications," *Progress In Electromagnetics Research C*, Vol. 45, 137–150, 2013.
11. Sankaranarayanan, D., D. Venkatakiran, and B. Mukherjee, "A novel compact fractal ring based cylindrical dielectric resonator antenna for ultra wideband application," *Progress In Electromagnetics Research C*, Vol. 67, 71–83, 2016.
12. Susila, M., T. Rama Rao, and A. Gupta, "A novel smiley fractal antenna (SFA) design and development for UWB wireless applications," *Progress In Electromagnetics Research C*, Vol. 54, 171–178, 2014.
13. Kaka, A. O. and M. Toycan, "Modified hexagonal Sierpinski gasket-based antenna design with multiband and miniaturized characteristics for UWB wireless communication," *Turkish Journal of Electrical Engineering and Computer Sciences*, Vol. 24, No. 2, 464–473, 2016.
14. Lin, C.-C. and H.-R. Chuang, "A 3–12 GHz UWB planar triangular monopole antenna with ridged ground-plane," *Progress In Electromagnetics Research*, Vol. 83, 307–321, 2008.
15. Tizyi, H., F. Riouch, A. Tribak, A. Najid, and A. Mediavilla, "CPW and microstrip line-fed compact fractal antenna for UWB-RFID applications," *Progress In Electromagnetics Research C*, Vol. 65, 201–209, 2016.
16. Kumar, R. and S. Gaikwad, "On the design of nano-arm fractal antenna for UWB wireless applications," *Journal of Microwaves, Optoelectronics and Electromagnetic Applications*, Vol. 12, No. 1, fp158–fp172, 2013.
17. Madhav, B. T. P., D. S. Ram Kiran, V. Alekhya, M. Vani, T. Anilkumar, et al. "An asymmetric liquid crystal polymer based fractal slotted UWB monopole antenna with notch band characteristics," *Rasayan Journal of Chemistry*, Vol. 10, No. 3, 852–860, 2017.
18. Wang, F., F. Bin, Q. Sun, J. Fan, and H. Ye, "A compact UHF antenna based on complementary fractal technique," *IEEE Access*, 5,8049453, 21118–21125, 2017.
19. Hu, Z., Y. Hu, Y. Luo, and W. Xin, "A novel rectangle tree fractal UWB antenna with dual band-notched characteristics," *Progress In Electromagnetics Research C*, Vol. 68, 21–30, 2016.

20. Lincy, B. H., A. Srinivasan, and B. Rajalakshmi, "Wideband fractal microstrip antenna for wireless application," *IEEE Conference on Information and Communication Technologies, ICT 2013*, 6558191, 735–738, 2013.